Globally exponentially stable attitude observer with Earth velocity estimation

Pedro Batista, Carlos Silvestre, and Paulo Oliveira

Asian Journal of Control, vol. 21, no. 4, pp. 1409-1422, July 2019

https://doi.org/10.1002/asjc.2056

Asian Journal of Control, Vol. 00, No. 0, pp. 1–14, Month 2018
Published online in Wiley InterScience (www.interscience.wiley.com) DOI: 10.1002/asjc.0000

–Special Issue: Recent Advances on Data Fusion, Estimation in Navigation and Control–

Globally Exponentially Stable Attitude Observer with Earth Velocity Estimation

Pedro Batista, Carlos Silvestre, and Paulo Oliveira

ABSTRACT

This paper presents a novel observer for attitude estimation based on a triad of high-grade rate gyros aided by a body-fixed vector measurement of a constant inertial vector, departing from the majority of solutions that consider at least two of these vectors. A cascade approach is proposed, where the first block estimates a vector that is related to the angular velocity of the Earth and a second block estimates the attitude. While the topological characteristics are relaxed in the attitude observer so that global exponential stability is achieved, an additional stage is also devised that yields estimates directly on the special orthogonal group, preserving global convergence of the estimation error. Simulation results with realistic sensor noise were performed, including extensive Monte Carlo runs. These results illustrate the convergence of the proposed solution, as well as the achievable performance and robustness to sensor noise.

I. Introduction

1.1. Brief literature review

Attitude estimation has been a very hot topic of research for quite some time [1]. First and foremost, attitude estimates are required for the operation of robotic platforms, not only autonomous but also remotely-operated. Furthermore, the limitations induced by the topological constraints lead to a very interesting problem from a theoretical point of view. From a strict algebraic perspective, a solution for attitude determination has been derived long ago, see [2]. Nevertheless, it is very limited since it does not make use of all the information that is usually available, e.g. angular velocities, which can be employed for filtering purposes. In the survey [3] many different filtering solutions have been reviewed. As in many nonlinear problems, the extended Kalman filter (EKF) provided an earlier solution, see e.g. [4], [5], and [6]. However, the divergence due to the linearization errors of the EKF [3] has resulted in the pursuit of alternative estimators with convergence guarantees, in particular nonlinear observers, see e.g. [7], [8], [9], [10], [11], [12], [13], and references therein. Another interesting topic of research on attitude estimation is that of optimal filtering, see e.g. [14]. In [15] uncertainty ellipsoids were employed in the design of a deterministic attitude estimator. Previous work by the authors includes [16] and [17], where two different attitude estimators are proposed that avoid common problems of attitude estimation such as singularities, unwinding phenomena, or topological limitations for

Manuscript received March 13, 2018.

P. Batista is with the Institute for Systems and Robotics, Instituto Superior Técnico, Universidade de Lisboa, Portugal. Email: pbatista@isr.tecnico.ulisboa.pt Carlos Silvestre is with the Department of Electrical and Computer Engineering, Faculty of Science and Technology of the University of Macau. C. Silvestre is also with the Institute for Systems and Robotics, on leave from Instituto Superior Técnico, Universidade de Lisboa, Portugal. Email: cjs@isr.tecnico.ulisboa.pt Paulo Oliveira is with the Department of Mechanical Engineering, Instituto Superior Técnico, Universidade de Lisboa, Portugal. Email: pjcro@isr.tecnico.ulisboa.pt

This work was supported by the Fundação para a Ciência e a Tecnologia (FCT) through ISR under FCT [UID/EEA/50009/2013] and through the FCT project DECENTER [LISBOA-01-0145-FEDER-029605], funded by the Lisboa 2020 and PIDDAC programs by the Macao Science and Technology Development Fund under Grant FDCT/026/2017/A1, and by the University of Macau, Macao, China, under Project MYRG2018-00198-FST.

achieving global asymptotic stabilization, see [18] for a thorough discussion of these issues.

1.2. Topological constraints

As previously mentioned, the divergence of the EKF has originated the interest in the design of nonlinear observers. Among these, a popular trend is to explicitly consider the topological characteristics of the rotation matrices and impose, by construction, that the estimates are elements of the special orthogonal group $SO(3)$, see e.g. [9] and [12]. A clear advantage of this approach is that no further refinements are required, since the estimates are, by construction, rotation matrices. However, it is not so without its drawbacks, in particular those related to the existence of topological obstructions to achieve global stability by continuous feedback and the relatively small convergence speed near unstable and saddle points, as convincingly argued in [19]. A very recent approach successfully tackles this problem by employing hybrid observers, see [13], preserving the properties of the estimates. Other alternatives that achieve global asymptotic (or exponential) stability were proposed in [16, 17], [20], and [21], where the estimates are embedded in linear spaces, thus avoiding the topological obstructions to achieve global stability. The disadvantage is that the estimates of the observers are not restricted to the special orthogonal group $SO(3)$. Nevertheless, estimates on $SO(3)$ can be easily obtained, without loss of global convergence, and several approaches are available, see e.g. [20] and [21].

1.3. Contribution, novelty, and applications

The main contribution of this paper is the design and stability analysis of a novel attitude observer based on high-grade rate gyros and single body-fixed measurements of a constant inertial vector. The topological characteristics of some variables are lifted, embedding those in linear spaces, such that topological obstacles to global stability are avoided. A cascade structure is envisioned: i) in the first block, an estimate of the angular velocity of the Earth, expressed in body-fixed coordinates, is obtained; and ii) the second block estimates the attitude based on the estimate of the angular velocity of the Earth and an additional body-fixed vector measurement. Since the topological characteristics are not enforced in the observer, an additional result is also provided that yields estimates on $SO(3)$ and preserves global convergence. Preliminary work by the authors can be found in [22], where a solution to the problem addressed in this paper was first presented. This paper gives a comprehensive presentation of the solution that yields global convergence, with detailed derivations and proofs that had been omitted and a thorough performance evaluation resorting to Monte Carlo runs, including an additional scenario with aggressive maneuvers. Moreover, an additional result that provides estimates directly on $SO(3)$ is also derived. An alternative design was presented in [23], where the topological characteristics of $SO(3)$ are preserved but global convergence results are absent as a direct consequence.

For attitude estimation, the majority of solutions assume that there exist, at least, two body-fixed measurements of corresponding known constant vectors in inertial coordinates. Recent exceptions to this approach are presented in [24], [25], [26], [27], and [20], where time-varying reference vectors are considered and some form of persistency-of-excitation is required. Also with single vector observations, but considering only partial attitude estimation, solutions were proposed in [28] and [29]. In complete contrast with the aforementioned references, the single body-fixed vector that is assumed to be measured in this paper corresponds to a constant inertial vector. On the other hand, while only one vector is measured, a second body-fixed vector is dynamically estimated that actually corresponds to a constant known vector in inertial coordinates, thus ultimately providing the information that is required for attitude estimation, including the angular velocity of the Earth. Notice that, overall, the proposed idea is closer to the first, and more popular, class of solutions that require the existence of at least two body-fixed measurements of corresponding known constant vectors in inertial coordinates. However, only one body-fixed measurement is assumed available in this paper. Notice also that the designs presented in [24], [25], [26], [27], and [20] cannot be applied in the present case since the only vector observation that is directly available corresponds to a constant vector in inertial coordinates, which does not provide sufficient information for attitude estimation. Moreover, the traditional solutions that require at least two vector observations of two inertial vectors cannot be applied because only one vector observation is available in the considered scenario.

The proposed contribution requires, in comparison with traditional attitude estimation solutions, one less measurement of a constant inertial vector, and hence it has applicability in a myriad of scenarios. When there are strong magnetic anomalies, alternatives to the traditional magnetometer must be

considered. Mechanical gyro compasses, fibre optic gyro compasses, or more recently, gyro compasses based on the hemispherical resonator gyroscope, are examples of such alternatives. The proposed algorithm offers an alternative solution based on high-grade rate gyros, providing an integrated attitude estimation solution. On the other hand, in typical attitude solutions for vehicles that are not subject to strong accelerations, the accelerometer measurements are assumed to be close to the acceleration of gravity. For vehicles subject to strong accelerations, this is no longer valid, and the present paper offers an alternative solution since only one body-fixed vector observation is required, and thus the accelerometer measurements may be discarded.

1.4. INS initial alignment and the gyrocompass

The idea of using the angular velocity of the Earth about its own axis in navigation is not novel and the Earth's rotational velocity is a fundamental quantity in the alignment of mechanical gyrocompasses and strapdown inertial navigation systems [30]. Indeed, for the initial alignment of an inertial navigation system (INS), gyro compassing is usually performed. However, the initial alignment requires specific maneuvers, including positions where the platform is static. Moreover, from time to time, the INS needs to be re-calibrated, otherwise errors accumulate over time and become prohibitive. The novelty introduced in this paper is that the attitude of the platform is continuously estimated in closed-loop without any particular maneuver requirements. Furthermore, the estimate of the angular velocity of the Earth about its own axis is continuously updated, also in closed-loop, therefore eliminating the accumulation of errors over time. Gyro compasses are also related to the approach proposed in the paper in the sense that a gyro compass is a type of non-magnetic compass whose north-seeking function depends on the rotation around the axis of rotation of the Earth, see e.g. [31]. The use of a gyro compass is advantageous in that it is not affected by magnetic field anomalies and provides true North (geodetic North). To a certain extent, the approach proposed in this paper uses high-grade rate gyros to extract the angular velocity of the Earth, but it does so resorting to an estimation algorithm coupled with body-fixed measurements of any other vector whose inertial counterpart is constant and known.

1.5. Organization

The paper is organized as follows. The problem statement and the nominal system dynamics are introduced in Section II. The observer design and stability analysis are presented in Section III, whereas extensive simulation results are discussed in Section IV. Section V summarizes the main results of the paper.

II. Problem formulation and notation

2.1. Notation and properties

Throughout the paper the symbol $\mathbf{0}$ denotes a matrix of zeros and $\mathbf{I}$ an identity matrix, both of appropriate dimensions. A block diagonal matrix is represented by $\mathrm{diag}(\mathbf{A}_1, \ldots, \mathbf{A}_n)$. For $\mathbf{x} \in \mathbb{R}^3$ and $\mathbf{y} \in \mathbb{R}^3$, $\mathbf{x} \cdot \mathbf{y}$ and $\mathbf{x} \times \mathbf{y}$ represent the inner and cross products, respectively. For convenience, define also the transpose operator $(.)^T$, and notice that $\mathbf{x} \cdot \mathbf{y} = \mathbf{x}^T\mathbf{y}$, $\mathbf{x}, \mathbf{y} \in \mathbb{R}^3$. The Special Orthogonal Group is denoted by $SO(3) := \left\{\mathbf{X} \in \mathbb{R}^{3\times 3} : \mathbf{X}\mathbf{X}^T = \mathbf{X}^T\mathbf{X} = \mathbf{I} \wedge \det(\mathbf{X}) = 1\right\}$. In compact matrix form, $\mathbf{S}(\mathbf{x}) \in \mathbb{R}^{3\times 3}$ is the skew-symmetric matrix that encodes the cross product, i.e., $\mathbf{S}(\mathbf{x})\mathbf{y} = \mathbf{x} \times \mathbf{y} \quad \mathbf{x}, \mathbf{y} \in \mathbb{R}^3$. The following cross product and rotation properties are used extensively in the paper. The rotation matrix preserves the norm of a vector, i.e.,

$$\|\mathbf{R}\mathbf{a}\| = \|\mathbf{a}\|, \quad \mathbf{R} \in SO(3), \mathbf{a} \in \mathbb{R}^3. \tag{1}$$

Moreover, considering the cross product and the rotation of a vector as two binary operators (the rotation operands are an element of $SO(3)$ and a vector in $\mathbb{R}^3$), it follows that these are left-distributive over the cross product, i.e.,

$$(\mathbf{R}\mathbf{a}) \times (\mathbf{R}\mathbf{b}) = \mathbf{R}(\mathbf{a} \times \mathbf{b}), \quad \mathbf{R} \in SO(3), \mathbf{a}, \mathbf{b} \in \mathbb{R}^3. \tag{2}$$

2.2. Problem statement

Consider a robotic platform where a set of three, high-grade, orthogonally mounted rate gyros are available, in addition to another sensor, possibly inertial, that measures, in the reference frame of the platform, a vector that is constant in some inertial frame. Further consider that the rate gyros are sensitive to the angular velocity of the Earth about its own axis. Loosely speaking, the problem addressed in the paper is that of determining the attitude of the platform based on these sensor measurements.

To set the problem framework, let $\{I\}$ denote a local inertial coordinate reference frame, e.g. the North-East-Down (NED) coordinate frame with origin fixed

to some point of the Earth, and denote by $\{B\}$ the so-called body-fixed frame, attached to the platform. It is assumed, without loss of generality, that this is also the frame of the sensors. Notice that due to the rotation and curvature of the Earth, the NED coordinate frame is not truly inertial but for local navigation purposes it can be considered so. Let $\mathbf{R}(t) \in SO(3)$ denote the rotation matrix from $\{B\}$ to $\{I\}$, which satisfies

$$\dot{\mathbf{R}}(t) = \mathbf{R}(t)\mathbf{S}\left[\boldsymbol{\omega}(t)\right], \tag{3}$$

where $\boldsymbol{\omega}(t) \in \mathbb{R}^3$ is the angular velocity of $\{B\}$ with respect to $\{I\}$, expressed in $\{B\}$.

The measurements of the high-grade set of rate gyros are given by

$$\boldsymbol{\omega}_m(t) = \boldsymbol{\omega}(t) + \boldsymbol{\omega}_E(t), \tag{4}$$

where $\boldsymbol{\omega}_E(t) \in \mathbb{R}^3$ is the angular velocity of the Earth about its own axis, expressed in $\{B\}$. Denote by ${}^I\boldsymbol{\omega}_E \in \mathbb{R}^3$ the angular velocity of the Earth about its own axis expressed in $\{I\}$. Then,

$${}^I\boldsymbol{\omega}_E = \mathbf{R}(t)\boldsymbol{\omega}_E(t) \tag{5}$$

for all time t.

Let $\mathbf{m}(t) \in \mathbb{R}^3$ denote the measurements of the second sensor, which measures, in body-fixed coordinates, a vector that, when expressed in inertial coordinates, is assumed known and constant. Let ${}^I\mathbf{m} \in \mathbb{R}^3$ denote the inertial vector corresponding to $\mathbf{m}(t)$. Then, similarly to the angular velocity of the Earth about its own axis, one has

$${}^I\mathbf{m} = \mathbf{R}(t)\mathbf{m}(t) \tag{6}$$

for all time t.

Using (5) and (4) in (3), and considering (6), it is possible to write the nonlinear system

$$\begin{cases} \dot{\mathbf{R}}(t) = \mathbf{R}(t)\mathbf{S}\left[\boldsymbol{\omega}_m(t) - \mathbf{R}^T(t){}^I\boldsymbol{\omega}_E\right] \\ \mathbf{m}(t) = \mathbf{R}^T(t){}^I\mathbf{m} \end{cases}.$$

The problem considered in this paper is that of estimating $\mathbf{R}(t)$ based on $\boldsymbol{\omega}_m(t)$ and $\mathbf{m}(t)$, which are measured, and ${}^I\boldsymbol{\omega}_E$ and ${}^I\mathbf{m}$, which are assumed constant and known.

The following assumptions are considered throughout the paper.

Assumption 1 *The inertial vector ${}^I\mathbf{m}$ is not parallel to the angular velocity of the Earth ${}^I\boldsymbol{\omega}_E$, i.e., there exists a constant $c_v > 0$ such that*

$$\left\| {}^I\boldsymbol{\omega}_E \times {}^I\mathbf{m} \right\|^2 \geq c_v.$$

Assumption 2 *The signal $\boldsymbol{\omega}_m(t)$ and its derivative $\dot{\boldsymbol{\omega}}_m(t)$ are bounded for all time.*

The first assumption is standard since most attitude estimation solutions assume that there exist, at least two known non-parallel inertial vectors, which are measured in body-fixed coordinates. Yet, in this paper, one of the two vectors, $\boldsymbol{\omega}_E(t)$, is not even directly measured. Instead, it is also explicitly estimated. The second is a technical assumption that is evidently verified for all systems in practice, since one cannot have arbitrarily large angular velocities or angular accelerations. It is also a standard assumption in attitude estimation, see e.g. [8], [12], [25], and [21].

III. Observer design

This section presents the attitude observer design and stability analysis. First, an observer that yields estimates of the angular velocity of Earth about its own axis is detailed in Section 3.1. Then, an attitude observer that features globally exponentially stable error dynamics, fed by the sensor measurements and the estimates of the previous observer, is proposed in Section 3.2. Finally, some additional remarks are presented in Section 3.3.

3.1. Earth rotation observer

First, take the time derivative of the vector measurement $\mathbf{m}(t)$, which from (3) and (6) is given by

$$\dot{\mathbf{m}}(t) = -\mathbf{S}\left[\boldsymbol{\omega}(t)\right]\mathbf{m}(t). \tag{7}$$

Since the angular velocity $\boldsymbol{\omega}(t)$ is not directly available, substitute (4) in (7), which yields

$$\dot{\mathbf{m}}(t) = -\mathbf{S}\left[\boldsymbol{\omega}_m(t) - \boldsymbol{\omega}_E(t)\right]\mathbf{m}(t). \tag{8}$$

Take the time derivative $\boldsymbol{\omega}_E(t)$, which from (3) and (5) is given by

$$\dot{\boldsymbol{\omega}}_E(t) = -\mathbf{S}\left[\boldsymbol{\omega}(t)\right]\boldsymbol{\omega}_E(t). \tag{9}$$

Substituting (4) in (9) and recalling that the cross product of two parallel vectors is zero allows to write

$$\dot{\boldsymbol{\omega}}_E(t) = -\mathbf{S}\left[\boldsymbol{\omega}_m(t)\right]\boldsymbol{\omega}_E(t). \tag{10}$$

From (8) one is suggested that, with measurements of $\mathbf{m}(t)$ and $\boldsymbol{\omega}_m(t)$, it might be possible to estimate $\mathbf{m}(t) \times \boldsymbol{\omega}_E(t)$. This is indeed the case, as it is shown next.

Define $\mathbf{x}_1(t) := \mathbf{m}(t)$ and $\mathbf{x}_2(t) := \mathbf{m}(t) \times \boldsymbol{\omega}_E(t)$. Then, from (8) and (10) one may write

$$\begin{cases} \dot{\mathbf{x}}_1(t) = -\mathbf{S}\left[\boldsymbol{\omega}_m(t)\right]\mathbf{x}_1(t) - \mathbf{x}_2(t) \\ \dot{\mathbf{x}}_2(t) = -\mathbf{S}\left[\boldsymbol{\omega}_m(t) - \boldsymbol{\omega}_E(t)\right]\mathbf{x}_2(t) \end{cases}. \tag{11}$$

The form of the time derivative of $\mathbf{x}_2(t)$ in (11) is undesirable since it still depends on $\boldsymbol{\omega}_E(t)$, when one has chosen to estimate $\mathbf{m}(t) \times \boldsymbol{\omega}_E(t)$ at this time. Consider as an orthonormal basis

$$\mathcal{B} := \left\{ \frac{\mathbf{x}_1(t)}{\|\mathbf{x}_1(t)\|}, \frac{\mathbf{x}_2(t)}{\|\mathbf{x}_2(t)\|}, \frac{\mathbf{x}_1(t) \times \mathbf{x}_2(t)}{\|\mathbf{x}_1(t) \times \mathbf{x}_2(t)\|} \right\}. \tag{12}$$

Notice that this set is always well-defined under Assumption 1. In order to eliminate the explicit dependence of $\dot{\mathbf{x}}_2(t)$ on $\boldsymbol{\omega}_E(t)$, one can decompose $\mathbf{S}\left[\boldsymbol{\omega}_E(t)\right]\mathbf{x}_2(t) = \boldsymbol{\omega}_E(t) \times \mathbf{x}_2(t)$ using the orthonormal basis (12), which gives

$$\mathbf{S}\left[\boldsymbol{\omega}_E(t)\right]\mathbf{x}_2(t) = A_{21}\mathbf{x}_1(t) + A_{22}\mathbf{S}\left[\mathbf{x}_1(t)\right]\mathbf{x}_2(t), \tag{13}$$

with

$$A_{21} := \frac{\left\|{}^I\boldsymbol{\omega}_E\right\|^2 \left\|{}^I\mathbf{m}\right\|^2 - \left({}^I\boldsymbol{\omega}_E \cdot {}^I\mathbf{m}\right)^2}{\left\|{}^I\mathbf{m}\right\|^2}$$

and

$$A_{22} := \frac{\left({}^I\boldsymbol{\omega}_E \cdot {}^I\mathbf{m}\right)\left\|{}^I\mathbf{m} \times {}^I\boldsymbol{\omega}_E\right\|^2}{\left\|{}^I\mathbf{m} \times \left({}^I\mathbf{m} \times {}^I\boldsymbol{\omega}_E\right)\right\|^2},$$

see Appendix A for the computations. Thus, the system dynamics (11) can be rewritten as

$$\begin{cases} \dot{\mathbf{x}}_1(t) = -\mathbf{S}\left[\boldsymbol{\omega}_m(t)\right]\mathbf{x}_1(t) - \mathbf{x}_2(t) \\ \dot{\mathbf{x}}_2(t) = A_{21}\mathbf{x}_1(t) - \mathbf{S}\left[\boldsymbol{\omega}_m(t) - A_{22}\mathbf{x}_1(t)\right]\mathbf{x}_2(t) \end{cases}. \tag{14}$$

Consider the Luenberger-like observer for (14) given by

$$\begin{cases} \dot{\hat{\mathbf{x}}}_1(t) = & -\mathbf{S}\left[\boldsymbol{\omega}_m(t)\right]\hat{\mathbf{x}}_1(t) - \hat{\mathbf{x}}_2(t) \\ & +\alpha_1\left[\mathbf{x}_1(t) - \hat{\mathbf{x}}_1(t)\right] \\ \dot{\hat{\mathbf{x}}}_2(t) = & A_{21}\mathbf{x}_1(t) - \mathbf{S}\left[\boldsymbol{\omega}_m(t) - A_{22}\mathbf{x}_1(t)\right]\hat{\mathbf{x}}_2(t) \\ & -\alpha_2\left[\mathbf{x}_1(t) - \hat{\mathbf{x}}_1(t)\right] \end{cases}, \tag{15}$$

where $\hat{\mathbf{x}}_1(t) \in \mathbb{R}^3$ and $\hat{\mathbf{x}}_2(t) \in \mathbb{R}^3$ correspond to the estimates of $\mathbf{x}_1(t)$ and $\mathbf{x}_2(t)$, respectively, and $\alpha_1 \in \mathbb{R}^+$ and $\alpha_2 \in \mathbb{R}^+$ are positive observer gains. Notice that, in order to achieve linear error dynamics, $\mathbf{x}_1(t)$ was employed in some of the terms of (15) rather than $\hat{\mathbf{x}}_1(t)$. Let $\tilde{\mathbf{x}}_1(t) := \mathbf{x}_1(t) - \hat{\mathbf{x}}_1(t)$ and $\tilde{\mathbf{x}}_2(t) := \mathbf{x}_2(t) - \hat{\mathbf{x}}_2(t)$ denote the estimation errors. Then, from (14) and (15) one may write the error dynamics

$$\begin{cases} \dot{\tilde{\mathbf{x}}}_1(t) = & -\left(\alpha_1\mathbf{I} + \mathbf{S}\left[\boldsymbol{\omega}_m(t)\right]\right)\tilde{\mathbf{x}}_1(t) - \tilde{\mathbf{x}}_2(t) \\ \dot{\tilde{\mathbf{x}}}_2(t) = & \alpha_2\tilde{\mathbf{x}}_1(t) - \mathbf{S}\left[\boldsymbol{\omega}_m(t) - A_{22}\mathbf{x}_1(t)\right]\tilde{\mathbf{x}}_2(t) \end{cases}. \tag{16}$$

The following theorem addresses the stability and convergence properties of (16).

Theorem 1 *Consider the state observer (15) and suppose that the observer gains α_1 and α_2 are positive. Further suppose that Assumptions 1 and 2 hold. Then, the origin of the error dynamics (16) is a globally exponentially stable equilibrium point.*

Proof The proof is in Appendix B.

The observer (15) allows to estimate the component of the angular velocity of the Earth that is orthogonal to the vector measurement $\mathbf{m}(t)$. This is sufficient to obtain an algebraic estimate of the rotation matrix $\mathbf{R}(t)$, as at this point one has access to two vectors in body-fixed coordinates, $\mathbf{m}(t)$ and $\mathbf{m}(t) \times \boldsymbol{\omega}_E(t)$ whose counterparts in inertial coordinates are also available, given by ${}^I\mathbf{m}$ and ${}^I\mathbf{m} \times {}^I\boldsymbol{\omega}_E$, respectively. However, that is not sufficient to obtain a filtered estimate of the rotation matrix since the complete angular velocity of the Earth is required, not just the component orthogonal to $\mathbf{m}(t)$. Nevertheless, one already has all the elements that allow to reconstruct the angular velocity of the Earth, as established in the following proposition.

Proposition 1 *Consider the estimates $\hat{\mathbf{x}}_1(t)$ and $\hat{\mathbf{x}}_2(t)$ given by the state observer (15) and define an estimate of the angular velocity of the Earth as*

$$\hat{\boldsymbol{\omega}}_E(t) = W_{e1}\hat{\mathbf{x}}_1(t) + W_{e2}\hat{\mathbf{x}}_1(t) \times \hat{\mathbf{x}}_2(t), \tag{17}$$

where

$$W_{e1} := \frac{{}^I\mathbf{m} \cdot {}^I\boldsymbol{\omega}_E}{\left\|{}^I\mathbf{m}\right\|^2}$$

and

$$W_{e2} := \frac{\left({}^I\mathbf{m} \cdot {}^I\boldsymbol{\omega}_E\right)^2 - \left\|{}^I\mathbf{m}\right\|^2\left\|{}^I\boldsymbol{\omega}_E\right\|^2}{\left\|{}^I\mathbf{m} \times \left({}^I\boldsymbol{\omega}_E \times {}^I\mathbf{m}\right)\right\|^2}.$$

Denote by $\tilde{\boldsymbol{\omega}}_E(t) := \boldsymbol{\omega}_E(t) - \hat{\boldsymbol{\omega}}_E(t)$ the estimation error of the angular velocity of the Earth. Then, under the conditions of Theorem 1, $\tilde{\boldsymbol{\omega}}_E(t)$ converges exponentially fast to zero for all initial conditions $\hat{\mathbf{x}}_1(t_0)$ and $\hat{\mathbf{x}}_2(t_0)$.

Proof The proof is in Appendix C.

3.2. Attitude observer

In the previous section an observer was proposed that gives filtered estimates of two vectors in body-fixed coordinates, $\hat{\mathbf{m}}(t)$ and $\hat{\mathbf{x}}_2(t)$, whose counterparts in inertial coordinates, i.e., ${}^I\mathbf{m}$ and ${}^I\mathbf{m} \times {}^I\boldsymbol{\omega}_E$, respectively, are also known. In addition, a filtered estimate of the angular velocity of the Earth was also obtained. In this section, the latter is used to drive the dynamics of a filtered estimate of the rotation matrix, while the two vectors in body-fixed coordinates, along with their counterparts in inertial coordinates, are used in the error injection term to drive the estimation error to zero. The overall structure of the cascade observer is depicted in Fig. 1. Notice that, while the information of the angular velocity of the Earth is not important *per se*, it is vital to estimate the attitude within the problem framework that is proposed in this paper.

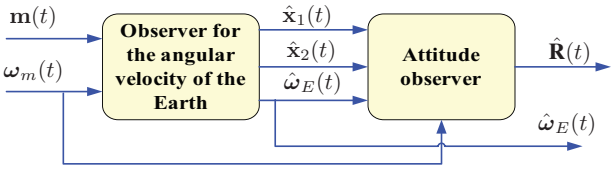

Fig. 1. Structure of the cascade attitude observer

It is important to remark that, given that estimates of body-fixed vectors whose inertial counterparts are now available, any vector-based attitude observer could be employed, provided that it is robust to exponentially decaying perturbations. One such design is provided in [16] and it is employed in this section with the necessary adaptations. The presentation is here streamlined and further details can be found in [16].

First, substitute (4) in (3), which gives

$$\dot{\mathbf{R}}(t) = \mathbf{R}(t)\mathbf{S}\left[\boldsymbol{\omega}_m(t) - \boldsymbol{\omega}_E(t)\right]. \tag{18}$$

Consider a column representation of the rotation matrix $\mathbf{R}(t)$ given by

$$\mathbf{z}_2(t) = \begin{bmatrix} \mathbf{r}_1(t) \\ \mathbf{r}_2(t) \\ \mathbf{r}_3(t) \end{bmatrix} \in \mathbb{R}^9,$$

where

$$\mathbf{R}(t) = \begin{bmatrix} \mathbf{r}_1^T(t) \\ \mathbf{r}_2^T(t) \\ \mathbf{r}_3^T(t) \end{bmatrix}, \ \mathbf{r}_i(t) \in \mathbb{R}^3, \ i = 1, \ldots, 3.$$

Then, from (18), it follows that

$$\dot{\mathbf{z}}_2(t) = -\mathbf{S}_3\left[\boldsymbol{\omega}_m(t) - \boldsymbol{\omega}_E(t)\right]\mathbf{z}_2(t),$$

where

$$\mathbf{S}_3(\mathbf{x}) := \operatorname{diag}\left(\mathbf{S}(\mathbf{x}), \mathbf{S}(\mathbf{x}), \mathbf{S}(\mathbf{x})\right) \in \mathbb{R}^{9\times 9}, \ \mathbf{x} \in \mathbb{R}^3.$$

Let

$${}^I\mathbf{m} = \begin{bmatrix} {}^Ix_{11} \\ {}^Ix_{12} \\ {}^Ix_{13} \end{bmatrix},$$

$${}^I\mathbf{m} \times {}^I\boldsymbol{\omega}_E = \begin{bmatrix} {}^Ix_{21} \\ {}^Ix_{22} \\ {}^Ix_{23} \end{bmatrix},$$

and

$${}^I\mathbf{m} \times \left({}^I\mathbf{m} \times {}^I\boldsymbol{\omega}_E\right) = \begin{bmatrix} {}^Ix_{31} \\ {}^Ix_{32} \\ {}^Ix_{33} \end{bmatrix}.$$

Notice that

$${}^I\mathbf{m} \times {}^I\boldsymbol{\omega}_E = \mathbf{R}(t)\mathbf{x}_2(t) \tag{19}$$

and

$${}^I\mathbf{m} \times \left({}^I\mathbf{m} \times {}^I\boldsymbol{\omega}_E\right) = \mathbf{R}(t)\left[\mathbf{x}_1(t) \times \mathbf{x}_2(t)\right]. \tag{20}$$

From (6), (19), and (20) it is possible to write

$$\mathbf{y}(t) = \mathbf{C}_2\mathbf{z}_2(t),$$

where

$$\mathbf{y}(t) = \begin{bmatrix} \mathbf{x}_1(t) \\ \mathbf{x}_2(t) \\ \mathbf{x}_1(t) \times \mathbf{x}_2(t) \end{bmatrix} \in \mathbb{R}^9$$

and

$$\mathbf{C}_2 = \begin{bmatrix} {}^Ix_{11} & 0 & 0 & {}^Ix_{12} & 0 & 0 & {}^Ix_{13} & 0 & 0 \\ 0 & {}^Ix_{11} & 0 & 0 & {}^Ix_{12} & 0 & 0 & {}^Ix_{13} & 0 \\ 0 & 0 & {}^Ix_{11} & 0 & 0 & {}^Ix_{12} & 0 & 0 & {}^Ix_{13} \\ {}^Ix_{21} & 0 & 0 & {}^Ix_{22} & 0 & 0 & {}^Ix_{23} & 0 & 0 \\ 0 & {}^Ix_{21} & 0 & 0 & {}^Ix_{22} & 0 & 0 & {}^Ix_{23} & 0 \\ 0 & 0 & {}^Ix_{21} & 0 & 0 & {}^Ix_{22} & 0 & 0 & {}^Ix_{23} \\ {}^Ix_{31} & 0 & 0 & {}^Ix_{32} & 0 & 0 & {}^Ix_{33} & 0 & 0 \\ 0 & {}^Ix_{31} & 0 & 0 & {}^Ix_{32} & 0 & 0 & {}^Ix_{33} & 0 \\ 0 & 0 & {}^Ix_{31} & 0 & 0 & {}^Ix_{32} & 0 & 0 & {}^Ix_{33} \end{bmatrix}.$$

Notice that, under Assumption 1, $\mathbf{C}_2$ has full rank.

Consider the Luenberger-like attitude observer given by

$$\begin{aligned} \dot{\hat{\mathbf{z}}}_2(t) \ &= \ -\mathbf{S}_3\left[\boldsymbol{\omega}_m(t) - \hat{\boldsymbol{\omega}}_E(t)\right]\hat{\mathbf{z}}_2(t) \\ &\quad +\mathbf{C}_2^T\mathbf{Q}^{-1}\left[\hat{\mathbf{y}}(t) - \mathbf{C}_2\hat{\mathbf{z}}_2(t)\right], \end{aligned} \tag{21}$$

where $\mathbf{Q} = \mathbf{Q}^T \in \mathbb{R}^{9\times 9}$ is a positive definite matrix and

$$\hat{\mathbf{y}}(t) = \begin{bmatrix} \hat{\mathbf{x}}_1(t) \\ \hat{\mathbf{x}}_2(t) \\ \hat{\mathbf{x}}_1(t) \times \hat{\mathbf{x}}_2(t) \end{bmatrix}.$$

Define the error variable $\tilde{\mathbf{z}}_2(t) = \mathbf{z}_2(t) - \hat{\mathbf{z}}_2(t)$. Then, the observer error dynamics are given by

$$\dot{\tilde{\mathbf{z}}}_2(t) = \left(\mathbf{A}_2(t) - \mathbf{S}_3\left[\tilde{\boldsymbol{\omega}}_E(t)\right]\right)\tilde{\mathbf{z}}_2(t) + \mathbf{u}_2(t), \quad (22)$$

where

$$\mathbf{A}_2(t) = -\mathbf{C}_2^T\mathbf{Q}^{-1}\mathbf{C}_2 - \mathbf{S}_3\left[\boldsymbol{\omega}(t)\right]$$

and

$$\mathbf{u}_2(t) = \mathbf{S}_3\left(\tilde{\boldsymbol{\omega}}_E(t)\right)\mathbf{z}_2(t) + \mathbf{C}_2^T\mathbf{Q}^{-1}\tilde{\mathbf{y}}(t),$$

with $\tilde{\mathbf{y}}(t) := \mathbf{y}(t) - \hat{\mathbf{y}}(t)$.

The following theorem is the main result of this section.

Theorem 2 *Consider the attitude observer* (21)*, where the estimates of the vector observations,* $\hat{\mathbf{y}}(t)$*, are obtained using the state observer* (15) *and the estimates of the angular velocity of the Earth,* $\hat{\boldsymbol{\omega}_E}(t)$*, are given by* (17)*. Then, under the conditions of Theorem 1, and assuming that* $\mathbf{Q}$ *is a positive definite matrix, it follows that the origin of the error dynamics* (22) *is a globally exponentially stable equilibrium point.*

Proof The proof is in Appendix E.

3.3. Further discussion

3.3.1. Additional vector measurements

In this paper only one body-fixed vector measurement was considered, in addition to the rate-gyro measurements. However, the design can be extended to include an arbitrary number of body-fixed vector measurements. One way would be to replicate the state observer (15), which would allow to obtain filtered estimates of each of those body-fixed vectors, as well as estimates of the components of the angular velocity of the Earth orthogonal to each of those body-fixed vectors. An overall estimate of the angular velocity of the Earth could then be obtained, in an algebraic and computationally efficient way, as the solution of an optimization problem, given all those estimates. Another way would be to include, in a single observer, each of those body-fixed vector estimates, as well as the angular velocity of the Earth, not just the orthogonal component. The attitude observer, given all the body-fixed vector estimates, is a straightforward generalization, see [16]. Here, the case with less number of measurements was preferred since it is indeed the most challenging from the theoretical point of view and, in all truth, the most interesting from the practical point of view since it requires a smaller number of sensors.

3.3.2. Estimates in $SO(3)$

The estimates of the rotation matrix provided by the attitude observer (21) do not necessarily belong to $SO(3)$, although they converge asymptotically to elements of $SO(3)$. Indeed, the rotation estimate

$$\hat{\mathbf{R}}(t) = \begin{bmatrix} \hat{\mathbf{r}}_1^T(t) \\ \hat{\mathbf{r}}_2^T(t) \\ \hat{\mathbf{r}}_3^T(t) \end{bmatrix},$$

with $\hat{\mathbf{z}}_2(t) = \begin{bmatrix} \hat{\mathbf{r}}_1^T(t) & \hat{\mathbf{r}}_3^T(t) & \hat{\mathbf{r}}_3^T(t) \end{bmatrix}^T$, does not necessarily belong to $SO(3)$. As previously discussed, this is a choice of design that allows one to achieve global stability. Indeed, it can be seen as a lifting technique that allows one to obtain globally exponentially stable error dynamics by lifting the topological constraints and it has been used in the past, see e.g. [16], [17], [20], [21], and [32]. Nevertheless, one can still obtain explicit estimates on $SO(3)$ and there exist several methods in the literature to obtain such constructs from the estimates provided by (21), see e.g. [16], [20], [21], and [32] for successful alternatives. Next, an additional result is provided with one of these alternatives, which is closely related to the solution proposed in [20].

Theorem 3 *Consider the estimate* $\hat{\mathbf{R}}(t)$ *obtained from the attitude observer* (21)*, under the conditions of Theorem 2, with GES error dynamics. Further suppose that the initial estimate satisfies* $\hat{\mathbf{R}}(t_0) \in SO(3)$ *and fix* $0 < \epsilon < 1$*. Define a new attitude estimate* $\hat{\mathbf{R}}_f(t)$ *of the rotation matrix* $\mathbf{R}(t)$ *as follows*

- *if* $\left\|\hat{\mathbf{R}}^T(t)\hat{\mathbf{R}}(t) - \mathbf{I}\right\| \leq \epsilon$*, then*

$$\hat{\mathbf{R}}_f(t) = \arg\min_{\mathbf{X}(t)\in SO(3)} \left\|\mathbf{X}(t) - \hat{\mathbf{R}}(t)\right\|$$

- *if* $\left\|\hat{\mathbf{R}}^T(t)\hat{\mathbf{R}}(t) - \mathbf{I}\right\| > \epsilon$*, then*

$$\dot{\hat{\mathbf{R}}}_f(t) = \hat{\mathbf{R}}_f(t)\mathbf{S}\left(\boldsymbol{\omega}(t) - \hat{\boldsymbol{\omega}}_E(t)\right).$$

Then,

1. $\hat{\mathbf{R}}_f(t) \in SO(3)$*;*
2. *there exists* t_s *such that* $\left\|\hat{\mathbf{R}}^T(t)\hat{\mathbf{R}}(t) - \mathbf{I}\right\| \leq \epsilon$ *for all* $t \geq t_s$ *and therefore* $\hat{\mathbf{R}}_f(t)$ *corresponds to the projection on* $SO(3)$ *of* $\hat{\mathbf{R}}(t)$ *for all* $t \geq t_s$*; and*
3. *the error* $\tilde{\mathbf{R}}_f(t) := \left\|\mathbf{R}(t) - \hat{\mathbf{R}}_f(t)\right\|$ *is bounded and*

$$\lim_{t\to\infty} \left\|\tilde{\mathbf{R}}_f(t)\right\| = 0.$$

Moreover, the convergence is exponentially fast.

Proof The proof is essentially identical to [20, Theorem 7] in spite of the different system dynamics when $\left\|\hat{\mathbf{R}}^T(t)\hat{\mathbf{R}}(t)-\mathbf{I}\right\| > \epsilon$. Since in this case it is still ensured that $\hat{\mathbf{R}}_f(t) \in SO(3)$ for all $t \geq t_0$, all the remaining steps of the proof apply.

3.3.3. Computational requirements

The solution proposed in this paper, depicted in Fig. 1, corresponds to a cascade structure of two Luenberger-like observers, with constant gains. Hence, the proposed observer has minimal computational cost. The first observer has six states, whereas the second observer has nine states. To estimate the angular velocity of the Earth, which is essential to drive the attitude dynamics, as it can be seen from (18), six states are necessary, three corresponding to the measured quantity $\mathbf{m}(t)$ and another three corresponding to the estimate of the second body-fixed vector $\mathbf{x}_2(t)$. The number of states of the second observer could be reduced if a different representation of the attitude was chosen. As previously mentioned, other attitude observers could have been devised for the second block, with different advantages and disadvantages. The one chosen in this paper allows to obtain globally exponentially stable error dynamics, a key property in this case since: i) initialization close to the true value is impossible and; ii) the initial error may be arbitrarily large.

IV. Simulation results

To illustrate the performance of the proposed solution, numerical simulations are performed and discussed in this section. The local inertial frame was considered as the NED frame, centered at a latitude of $\varphi = 38.7138°$North, a longitude of $\psi = 9.1394°$West, and at sea level. The norm of the angular velocity of the Earth was set to $\left\|{}^I\boldsymbol{\omega}_E\right\| = 7.2921150 \times 10^{-5}$ rad/s, which corresponds approximately to 15 degrees per hour. Thus, in the NED frame, one has ${}^I\boldsymbol{\omega}_E = \left\|{}^I\boldsymbol{\omega}_E\right\| \begin{bmatrix} \cos\varphi & 0 & -\sin\varphi \end{bmatrix}^T$. As for the vector measurement $\mathbf{m}(t)$, it is assumed that magnetic field measurements are available. However, any other inertial vector could have been considered. In this case, ${}^I\mathbf{m}$ was set according to the 11^{th} generation of International Geomagnetic Reference Field for the latitude, longitude, and altitude previously described. Notice that, with this choice, Assumption 1 is satisfied.

Table 1. Observer gains for (15)

Time interval (s)	α_1	α_2
$[0, 60[$	100	10
$[60, 120[$	10	1
$[120, 240[$	5	10^{-1}
$[240, 300[$	5	5×10^{-2}
$[300, 600[$	5	25×10^{-3}
$[600, 720[$	2.5	10×10^{-3}
$[720, +\infty[$	2.5	5×10^{-3}

The initial attitude of the platform was set to $\mathbf{R}(0) = \mathbf{I}$ and the evolution of the angular velocity is given by

$$\boldsymbol{\omega}(t) = \begin{bmatrix} 5\frac{\pi}{180}\sin\left(\frac{2\pi}{60}t\right) \\ \frac{\pi}{180}\sin\left(\frac{2\pi}{180}t\right) \\ -2\frac{\pi}{180}\sin\left(\frac{2\pi}{300}t\right) \end{bmatrix} \text{(rad/s)}.$$

In order to demonstrate the robustness of the proposed solutions to sensor measurement errors, the measurements of the magnetometer were assumed to be corrupted by zero-mean white Gaussian noise, with standard deviation of 150 nT, which corresponds to the worst case specification for the standard deviation of the noise of the triaxial magnetometer of the nanoIMU NA02-0150F50. The rate gyro measurements are also to be corrupted by noise, characterized by an angle random walk of $4°/\text{hr}/\sqrt{\text{Hz}}$, which corresponds to the KVH DSP-3000 fiber optic gyro. A sampling frequency of 100 Hz was considered and the fourth-order Runge-Kutta method was employed in the simulations.

In order to ensure both fast convergence speed and good steady-state performance, a set of piece-wise constant gains was chosen for the first block. This does not impact on the stability of the error dynamics since a finite set of transitions is considered. These gains are described in Table 1. As for the second block, its gain was set to

$$\mathbf{Q} = 10^5\mathbf{C}_2\mathbf{Q}_D\mathbf{C}_2^T,$$

with

$$\mathbf{Q}_D = \text{diag}\left(\frac{20}{\|{}^I\mathbf{m}\|}\mathbf{I}, \frac{2\times10^{-2}}{\|{}^I\boldsymbol{\omega}_E\times{}^I\mathbf{m}\|}\mathbf{I}, \frac{10^3}{\|{}^I\mathbf{m}\times({}^I\boldsymbol{\omega}_E\times{}^I\mathbf{m})\|}\mathbf{I}\right).$$

These gains were chosen empirically, although the relative gains of the second observer are related to the error noise of its observations. The initial estimates of the first observer were set to zero, while the initial attitude estimate was set to $\hat{\mathbf{R}}(0) = \text{diag}(-1, -1, 1)$.

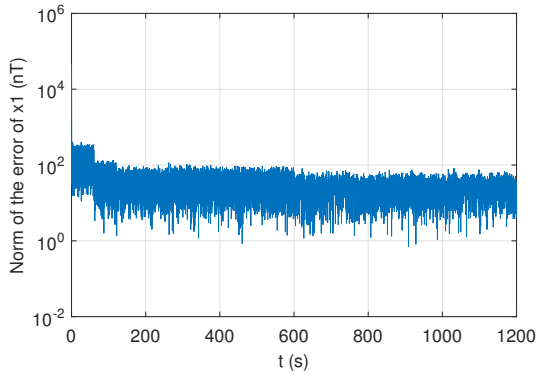

(a) $\|\tilde{\mathbf{x}}_1(t)\|$

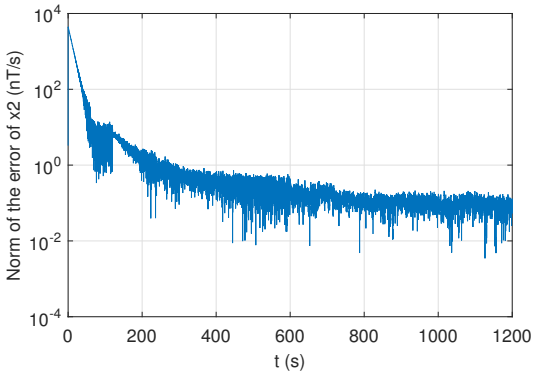

(b) $\|\tilde{\mathbf{x}}_2(t)\|$

Fig. 2. Initial convergence of the errors of (15)

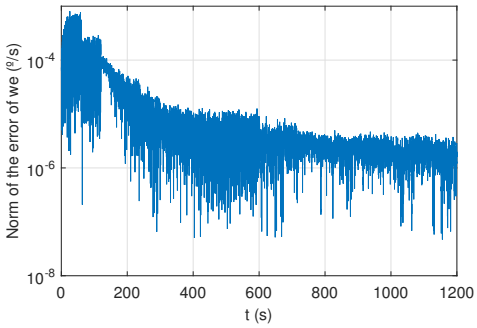

Fig. 3. Initial convergence of $\|\tilde{\boldsymbol{\omega}}_E(t)\|$

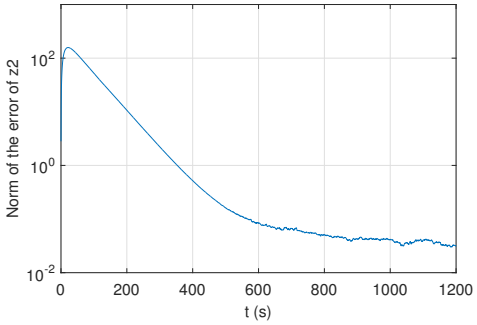

Fig. 4. Initial convergence of the error $\tilde{\mathbf{z}}_2(t)$

Table 2. Standard deviation of the steady-state error - the mean value of the standard deviation for each element of the error vectors is shown

Variable	Standard deviation
$\tilde{\mathbf{x}}_1(t)$ (nT)	17.7
$\tilde{\mathbf{x}}_2(t)$ (nT/s)	0.044
$\tilde{\boldsymbol{\omega}}_E(t)$ (°/hour)	0.182
$\tilde{\mathbf{z}}_2(t)$	0.0069

The initial convergence of the norm of the errors $\tilde{\mathbf{x}}_1(t)$ and $\tilde{\mathbf{x}}_2(t)$ is depicted in Fig. 2. While the convergence of the observer is fast, different gains are required, as detailed in Table 1, in order to ensure an adequate steady-state level of error, as it will be detailed shortly. The initial convergence of the error $\tilde{\boldsymbol{\omega}}_E(t)$ is depicted in Fig. 3. Finally, the initial convergence of the attitude error, expressed as $\tilde{\mathbf{z}}_2(t)$, is shown in Fig. 4. These plots show that the error converges to a neighborhood of zero. In the absence of noise, the errors converge to zero.

To evaluate the performance of the attitude observer, the steady-state standard deviation of the errors is depicted in Table 2. These values should be compared to the magnitude of the corresponding variables, which is roughly 4.5×10^4 nT for $\mathbf{x}_1(t)$, 3.27 nT/s for $\mathbf{x}_2(t)$, and 15°/hour for $\boldsymbol{\omega}_E(t)$. Evidently, the observer achieves very good results. Finally, an additional error variable is defined as $\tilde{\mathbf{R}}(t) = \mathbf{R}^T(t)\hat{\mathbf{R}}_e(t)$, which corresponds to the rotation matrix error. Here, $\hat{\mathbf{R}}_e(t)$ corresponds to the projection of the obtained attitude estimate on $SO(3)$. Using the Euler angle-axis representation for the rotation error,

$$\begin{aligned}\tilde{\mathbf{R}}(t) &= \mathbf{I}\cos\left(\tilde{\theta}(t)\right) + \left[1-\cos\left(\tilde{\theta}(t)\right)\right]\tilde{\mathbf{d}}(t)\tilde{\mathbf{d}}^T(t) \\ &\quad -\mathbf{S}\left(\tilde{\mathbf{d}}(t)\right)\sin\left(\tilde{\theta}(t)\right), \end{aligned} \tag{23}$$

for this new error variable, the performance of the observer is easily identified from the evolution of $\tilde{\theta}$, which is depicted, after the initial transients fade out, in Fig. 5. The mean angle error, computed for $t \geq 2400$ s, is $0.586°$, which is again a very good result.

To better evaluate the performance of the proposed solutions, the Monte Carlo method was applied, and 1000 simulations were carried out with different, randomly generated noise signals. The mean angle

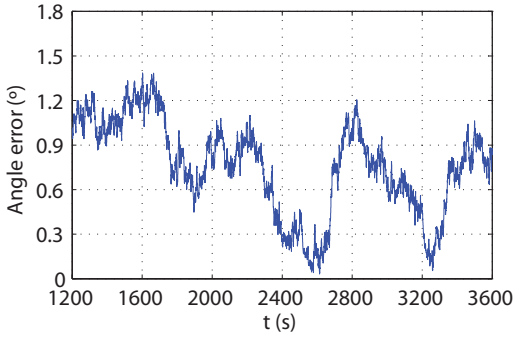

Fig. 5. Evolution of the angle error $\tilde{\theta}(t)$

error, using the Euler angle-axis representation (23), was computed for each simulation, for $t \geq 2400$ s, and averaged over the set of simulations. The corresponding mean angle error was $0.38°$.

In the simulations that were presented, the angular velocity of the body does not exceed $5°/s$ around each principal axis. Hence, it is only natural to ask if much higher angular velocities have any impact whatsoever in the convergence speed or steady-state performance of the proposed solution. As it turns out, the proposed solutions can effectively handle much higher velocities. To exemplify that situation, the previous simulation was modified considering an angular velocity 20 times higher than the previous one, as given by

$$\boldsymbol{\omega}(t) = \begin{bmatrix} 100\frac{\pi}{180}\sin\left(\frac{2\pi}{60}t\right) \\ 20\frac{\pi}{180}\sin\left(\frac{2\pi}{180}t\right) \\ -40\frac{\pi}{180}\sin\left(\frac{2\pi}{300}t\right) \end{bmatrix} \text{(rad/s)}\,.$$

This corresponds to very aggressive attitude maneuvers. All the other settings were kept as before. The initial convergence of the norm of the errors is very similar and hence it is omitted. This is to be expected. Indeed, as an example, the angular velocity $\boldsymbol{\omega}_m(t)$ appears in the dynamics of $\tilde{\mathbf{x}}_2(t)$, in (16), through the skew-symmetric term $-\mathbf{S}\left[\boldsymbol{\omega}_m(t)\right]\tilde{\mathbf{x}}_2(t)$, which preserves the norm of the error. Similar behaviors occur for the remaining errors, in particular $\tilde{\mathbf{x}}_1(t)$, $\tilde{\boldsymbol{\omega}}_E(t)$, and $\tilde{\mathbf{z}}_2(t)$, for the same reasons, and hence these are omitted. To evaluate the steady-state performance, the Monte Carlo method was applied, and 1000 simulations were carried out with different, randomly generated noise signals. The mean angle error, using the Euler angle-axis representation (23), was computed for each simulation, for $t \geq 2400$ s, and averaged over the set of simulations. The resulting mean angle error was $0.47°$, which corresponds only to a slight decrease in performance considering the very aggressive angular velocities that are considered.

V. Conclusions

This paper proposes a novel attitude estimation solution that is based solely on measurements of a single body-fixed vector and the angular velocity provided by a set of three high-grade rate gyros, sensitive to the angular velocity of the Earth about its own axis. In contrast with the existing the literature, the only observed inertial vector is constant. The key idea of the observer design, which is cascaded, is to obtain an estimate of a second vector in body-fixed coordinates that corresponds to a constant known vector in inertial coordinates and that also allows one to estimate the angular velocity of the Earth about its own axis. Additionally, the topological constraints are lifted so that there are no topological obstacles to achieve global convergence. The error is shown to converge globally exponentially fast to zero and an additional result provides estimates that are always on $SO(3)$, preserving the global convergence results. Simulations are presented, including Monte Carlo results, that illustrate the achievable performance of the proposed solution for different angular velocity envelopes, considering also realistic sensor noise.

REFERENCES

1. H. Fourati and D. B. (Eds.), *Multisensor Attitude Estimation: Fundamental Concepts and Applications*. CRC Press, 2011.
2. G. Wahba, "A Least Squares Estimate of Spacecraft Attitude," *SIAM Review*, vol. 7, no. 3, p. 409, Jul. 1965.
3. J. Crassidis, F. Markley, and Y. Cheng, "Survey of Nonlinear Attitude Estimation Methods," *Journal of Guidance, Control and Dynamics*, vol. 30, no. 1, pp. 12–28, Jan.-Feb. 2007.
4. J. Farrell, "Attitude Determination by Kalman Filter," *Automatica*, vol. 6, no. 5, pp. 419–430, 1970.
5. I. Bar-Itzhack and Y. Oshman, "Attitude Determination from Vector Observations: Quaternion Estimation," *IEEE Transactions on Aerospace and Electronic Systems*, vol. 321, no. 1, pp. 128–136, Jan. 1985.
6. A. Sabatini, "Quaternion-based extended Kalman filter for determining orientation by inertial and magnetic sensing," *IEEE Transactions on Biomedical Engineering*, vol. 53, no. 7, pp. 1346–1356, Jul. 2006.
7. H. Grip, T. Fossen, T. Johansen, and A. Saberi, "Attitude Estimation Using Biased Gyro and

Vector Measurements with Time-Varying Reference Vectors," *IEEE Transactions on Automatic Control*, vol. 57, no. 5, pp. 1332–1338, May 2012.
8. M.-D. Hua, "Attitude estimation for accelerated vehicles using GPS/INS measurements," *Control Engineering Practice*, vol. 18, no. 7, pp. 723–732, Jul. 2010.
9. H. Rehbinder and B. Ghosh, "Pose Estimation Using Line-Based Dynamic Vision and Inertial Sensors," *IEEE Transactions on Automatic Control*, vol. 48, no. 2, pp. 186–199, Feb. 2003.
10. A. Roberts and A. Tayebi, "On the Attitude Estimation of Accelerating Rigid-Bodies Using GPS and IMU Measurements," in *Proceedings of the 50th IEEE Conference on Decision and Control*, Orlando, USA, Dec. 2011.
11. A. Barrau and S. Bonnabel, "Intrinsic filtering on Lie groups with applications to attitude estimation," *IEEE Transactions on Automatic Control*, vol. 60, no. 2, pp. 436–449, Feb. 2015.
12. R. Mahony, T. Hamel, and J.-M. Pflimlin, "Nonlinear Complementary Filters on the Special Orthogonal Group," *IEEE Transactions on Automatic Control*, vol. 53, no. 5, pp. 1203–1218, Jun. 2008.
13. A. Soulaimane, B. Abdessameud and A. Tayebi, "Hybrid Attitude and Gyro-Bias Observer Design on $SO(3)$," *IEEE Transactions on Automatic Control*, vol. 62, no. 11, pp. 6044–6050, Nov. 2017.
14. M. Zamani, J. Trumpf, and R. Mahony, "Minimum-Energy Filtering for Attitude Estimation," *IEEE Transactions on Automatic Control*, vol. 58, no. 11, pp. 2917–2921, Nov. 2013.
15. A. Sanyal, T. Lee, M. Leok, and N. McClamroch, "Global optimal attitude estimation using uncertainty ellipsoids," *Systems & Control Letters*, vol. 57, pp. 236–245, 2008.
16. P. Batista, C. Silvestre, and P. Oliveira, "Globally Exponentially Stable Cascade Observers for Attitude Estimation," *Control Engineering Practice*, vol. 20, no. 2, pp. 148–155, Feb. 2012.
17. ——, "Sensor-based Globally Asymptotically Stable Filters for Attitude Estimation: Analysis, Design, and Performance Evaluation," *IEEE Transactions on Automatic Control*, vol. 57, no. 8, pp. 2095–2100, Aug. 2012.
18. D. Bernstein and S. Bhata, "A topological obstruction to continuous global stabilization of rotational motion and the unwinding phenomenon," *Systems & Control Letters*, vol. 39, no. 1, pp. 63–70, 2000.
19. N. Chaturvedi, A. Sanyal, and N. McClamroch, "Rigid-Body Attitude Control," *IEEE Control Systems Magazine*, vol. 31, no. 3, pp. 30–51, Jun. 2011.
20. P. Batista, C. Silvestre, and P. Oliveira, "A GES Attitude Observer with Single Vector Observations," *Automatica*, vol. 48, no. 2, pp. 388–395, Feb. 2012.
21. H. Grip, T. Fossen, T. Johansen, and A. Saberi, "Observers for interconnected nonlinear and linear systems," *Automatica*, vol. 48, no. 7, pp. 1339–1346, Jul. 2012.
22. P. Batista, C. Silvestre, and P. Oliveira, "Attitude and Earth Velocity Estimation - Part I: Globally Exponentially Stable Observer," in *Proceedings of the 53rd IEEE Conference on Decision and Control*, Los Angeles, USA, Dec. 2014, pp. 121–126.
23. ——, "Attitude and Earth Velocity Estimation - Part II: Observer on the Special Orthogonal Group," in *Proceedings of the 53rd IEEE Conference on Decision and Control*, Los Angeles, USA, Dec. 2014, pp. 127–132.
24. J. Kinsey and L. Whitcomb, "Adaptive Identification on the Group of Rigid Body Rotations and its Application to Precision Underwater Robot Navigation," *IEEE Transactions on Robotics*, vol. 23, no. 1, pp. 124–136, Feb. 2007.
25. J. Trumpf, R. Mahony, T. Hamel, and C. Lageman, "Analysis of Non-Linear Attitude Observers for Time-Varying Reference Measurements," *IEEE Transactions on Automatic Control*, vol. 57, no. 11, pp. 2789–2800, Nov. 2012.
26. A. Khosravian and M. Namvar, "Rigid Body Attitude Control Using a Single Vector Measurement and Gyro," *IEEE Transactions on Automatic Control*, vol. 57, no. 5, pp. 1273–1279, May 2012.
27. M. Namvar and F. Safaei, "Adaptive Compensation of Gyro Bias in Rigid-Body Attitude Estimation Using a Single Vector Measurement," *IEEE Transactions on Automatic Control*, vol. 58, no. 7, pp. 1816–1822, Jul. 2013.
28. W. Wu, Z. Zhou, R. Li, L. Yang, and H. Fourati, "Attitude determination using a single sensor observation: analytic quaternion solutions and property discussion," *IET Science, Measurement & Technology*, vol. 11, no. 6, pp. 731–739, Sep. 2017.
29. P. Batista, C. Silvestre, and P. Oliveira, "Partial attitude and rate gyro bias estimation: observability analysis, filter design, and performance evaluation," *International Journal of Control*, vol. 84, no. 5, pp. 895–903, May 2011.

30. D. Titterton and J. Weston, *Strapdown Inertial Navigation Systems*. The Institution of Electrical Engineers, 2004.
31. W. Rueckner, "Using a gyroscope to find true north - A lecture demonstration," *American Journal of Physics*, vol. 85, no. 3, pp. 228–231, Mar. 2017.
32. C. Belta and V. Kumar, "An SVD-Based Projection Method for Interpolation on SE(3)," *IEEE Transactions on Robotics and Automation*, vol. 18, no. 3, pp. 334–345, Jun. 2002.
33. H. Khalil, *Nonlinear Systems*, 3rd ed. Prentice Hall, 2001.
34. P. Ioannou and J. Sun, *Robust Adaptive Control*. Prentice Hall, 1995.
35. P. Batista, C. Silvestre, and P. Oliveira, "On the observability of linear motion quantities in navigation systems," *Systems & Control Letters*, vol. 60, no. 2, pp. 101–110, Feb. 2011.

A. Decomposition of $\boldsymbol{\omega}_E(t) \times \mathbf{x}_2(t)$

The decomposition of $\boldsymbol{\omega}_E(t) \times \mathbf{x}_2(t)$ in the orthonormal basis (12) is given by

$$\begin{aligned}\mathbf{S}\left[\boldsymbol{\omega}_E(t)\right]\mathbf{x}_2(t) = (\boldsymbol{\omega}_E(t)\times\mathbf{x}_2(t))\cdot\tfrac{\mathbf{x}_1(t)}{\|\mathbf{x}_1(t)\|}\tfrac{\mathbf{x}_1(t)}{\|\mathbf{x}_1(t)\|}\\ +(\boldsymbol{\omega}_E(t)\times\mathbf{x}_2(t))\cdot\tfrac{\mathbf{x}_2(t)}{\|\mathbf{x}_2(t)\|}\tfrac{\mathbf{x}_2(t)}{\|\mathbf{x}_2(t)\|}\\ +(\boldsymbol{\omega}_E(t)\times\mathbf{x}_2(t))\cdot\tfrac{\mathbf{x}_1(t)\times\mathbf{x}_2(t)}{\|\mathbf{x}_1(t)\times\mathbf{x}_2(t)\|}\tfrac{\mathbf{x}_1(t)\times\mathbf{x}_2(t)}{\|\mathbf{x}_1(t)\times\mathbf{x}_2(t)\|}.\end{aligned} \tag{24}$$

First, notice that all norms in (24) are actually constant since they correspond to norms of vectors expressed in body-fixed coordinates that, in inertial coordinates, are constant. Indeed, from (6) one has $\|\mathbf{x}_1(t)\| = \|\mathbf{m}(t)\| = \left\|\mathbf{R}^T(t)\,{}^I\mathbf{m}\right\| = \left\|{}^I\mathbf{m}\right\|$, and from (5) and (6) one may write

$$\begin{aligned}\|\mathbf{x}_2(t)\| &= \|\mathbf{m}(t)\times\boldsymbol{\omega}_E(t)\|\\ &= \left\|\left[\mathbf{R}^T(t)\,{}^I\mathbf{m}\right]\times\left[\mathbf{R}^T(t)\,{}^I\boldsymbol{\omega}_E\right]\right\|\\ &= \left\|\mathbf{R}^T(t)\left[{}^I\mathbf{m}\times{}^I\boldsymbol{\omega}_E\right]\right\|\\ &= \left\|{}^I\mathbf{m}\times{}^I\boldsymbol{\omega}_E\right\|\end{aligned}$$

and

$$\begin{aligned}\|\mathbf{x}_1(t)\times\mathbf{x}_2(t)\| &= \|\mathbf{m}(t)\times[\mathbf{m}(t)\times\boldsymbol{\omega}_E(t)]\|\\ &= \left\|\mathbf{m}(t)\times\left(\left[\mathbf{R}^T(t)\,{}^I\mathbf{m}\right]\times\left[\mathbf{R}^T(t)\,{}^I\boldsymbol{\omega}_E\right]\right)\right\|\\ &= \left\|\left[\mathbf{R}^T(t)\,{}^I\mathbf{m}\right]\times\left(\mathbf{R}^T(t)\left[{}^I\mathbf{m}\times{}^I\boldsymbol{\omega}_E\right]\right)\right\|\\ &= \left\|\mathbf{R}^T(t)\left[{}^I\mathbf{m}\times\left({}^I\mathbf{m}\times{}^I\boldsymbol{\omega}_E\right)\right]\right\|\\ &= \left\|{}^I\mathbf{m}\times\left({}^I\mathbf{m}\times{}^I\boldsymbol{\omega}_E\right)\right\|,\end{aligned}$$

where the properties (1) and (2) were used extensively. Next, notice that the second term of the sum in (24) is null since $\boldsymbol{\omega}_E(t)\times\mathbf{x}_2(t)$ is orthogonal to $\mathbf{x}_2(t)$. It remains to compute the other two inner products in (24). For the first term, using the vector triple product one may write

$$\begin{aligned}&(\boldsymbol{\omega}_E(t)\times\mathbf{x}_2(t))\cdot\mathbf{x}_1(t) =\\ &= (\boldsymbol{\omega}_E(t)\times[\mathbf{m}(t)\times\boldsymbol{\omega}_E(t)])\cdot\mathbf{m}(t)\\ &= \left(\|\boldsymbol{\omega}_E(t)\|^2\,\mathbf{m}(t) - [\boldsymbol{\omega}_E(t)\cdot\mathbf{m}(t)]\,\boldsymbol{\omega}_E(t)\right)\cdot\mathbf{m}(t)\\ &= \|\boldsymbol{\omega}_E(t)\|^2\,\|\mathbf{m}(t)\|^2 - [\boldsymbol{\omega}_E(t)\cdot\mathbf{m}(t)]^2.\end{aligned} \tag{25}$$

Substituting (5) and (6) in (25) and using (1) and

$$\mathbf{R}\mathbf{R}^T = \mathbf{I},\quad \mathbf{R}\in SO(3), \tag{26}$$

gives

$$(\boldsymbol{\omega}_E(t)\times\mathbf{x}_2(t))\cdot\mathbf{x}_1(t) = \left\|{}^I\boldsymbol{\omega}_E\right\|^2\left\|{}^I\mathbf{m}\right\|^2 - \left({}^I\boldsymbol{\omega}_E\cdot{}^I\mathbf{m}\right)^2.$$

For the last term of (24), use the Binet-Cauchy identity and the fact that $\boldsymbol{\omega}_E(t)$ is orthogonal to $\boldsymbol{\omega}_E(t)\times\mathbf{m}(t)$, which gives

$$\begin{aligned}&(\boldsymbol{\omega}_E(t)\times\mathbf{x}_2(t))\cdot[\mathbf{x}_1(t)\times\mathbf{x}_2(t)]\\ &= [\boldsymbol{\omega}_E(t)\cdot\mathbf{m}(t)]\,\|\mathbf{m}(t)\times\boldsymbol{\omega}_E(t)\|^2.\end{aligned} \tag{27}$$

Following the same reasoning as before, using (1), (2), (5), (6), and (26) allows one to rewrite (27) as

$$\begin{aligned}&(\boldsymbol{\omega}_E(t)\times\mathbf{x}_2(t))\cdot[\mathbf{x}_1(t)\times\mathbf{x}_2(t)]\\ &= \left({}^I\boldsymbol{\omega}_E\cdot{}^I\mathbf{m}\right)\left\|{}^I\mathbf{m}\times{}^I\boldsymbol{\omega}_E\right\|^2.\end{aligned}$$

This readily gives (13).

B. Proof of Theorem 1

Consider the compact error definition

$$\mathbf{z}_1(t) := \begin{bmatrix}\tilde{\mathbf{x}}_1(t)\\ \tilde{\mathbf{x}}_2(t)\end{bmatrix}\in\mathbb{R}^6$$

and notice that the error dynamics (16) can be written as the linear time-varying system

$$\dot{\mathbf{z}}_1(t) = \mathbf{A}_1(t)\mathbf{z}_1(t),$$

with

$$\mathbf{A}_1(t) := \begin{bmatrix}-(\alpha_1\mathbf{I}+\mathbf{S}\left[\boldsymbol{\omega}_m(t)\right]) & -\mathbf{I}\\ \alpha_2\mathbf{I} & -\mathbf{S}\left[\boldsymbol{\omega}_m(t) - A_{22}\mathbf{x}_1(t)\right]\end{bmatrix}.$$

Define the Lyapunov-like function

$$V\left(\mathbf{z}_1(t)\right) := \mathbf{z}_1^T(t)\mathbf{P}\mathbf{z}_1(t),$$

with

$$\mathbf{P} = \begin{bmatrix} \frac{1}{2}\mathbf{I} & \mathbf{0} \\ \mathbf{0} & \frac{1}{2\alpha_2}\mathbf{I} \end{bmatrix} \in \mathbb{R}^{6\times 6}.$$

Notice that $\mathbf{P}$ is, by construction and under the assumptions of the theorem, constant and positive definite. Therefore, using the Rayleigh-Ritz inequality, there exist $\gamma_1 > 0$ and $\gamma_2 > 0$ such that

$$\gamma_1 \left\|\mathbf{z}_1(t)\right\|^2 \leq V\left(\mathbf{z}_1(t)\right) \leq \gamma_2 \left\|\mathbf{z}_1(t)\right\|^2.$$

Next, take the time derivative of $V\left(\mathbf{z}_1(t)\right)$, which can be written as

$$\dot{V}\left(\mathbf{z}_1(t)\right) = -\mathbf{z}_1^T(t)\mathbf{C}_1^T\mathbf{C}_1\mathbf{z}_1(t) \leq 0,$$

with $\mathbf{C}_1 = \begin{bmatrix} \sqrt{\alpha_1}\mathbf{I} & \mathbf{0} \end{bmatrix} \in \mathbb{R}^{3\times 6}$. To show that the origin of the error dynamics (16) is a globally exponentially stable equilibrium point, it now suffices to show that the pair $(\mathbf{A}_1(t), \mathbf{C}_1)$ is uniformly completely observable, see [33, Example 8.11]. Since uniform complete observability is preserved under continuous output feedback, see [34, Lemma 4.8.1], uniform complete observability of the pair $(\mathbf{A}_1(t), \mathbf{C}_1)$ is equivalent to uniform complete observability of the pair $(\boldsymbol{\mathcal{A}}_1(t), \mathbf{C}_1)$, with

$$\begin{aligned} \boldsymbol{\mathcal{A}}_1(t) &= \mathbf{A}_1(t) - \mathbf{K}_1(t)\mathbf{C}_1 \\ &= \begin{bmatrix} \mathbf{0} & -\mathbf{I} \\ \mathbf{0} & -\mathbf{S}\left[\boldsymbol{\omega}_m(t) - A_{22}\mathbf{x}_1(t)\right] \end{bmatrix}, \end{aligned}$$

where

$$\mathbf{K}_1(t) = \frac{1}{\sqrt{\alpha_1}} \begin{bmatrix} -\left(\alpha_1\mathbf{I} + \mathbf{S}\left[\boldsymbol{\omega}_m(t)\right]\right) \\ \alpha_2\mathbf{I} \end{bmatrix} \in \mathbb{R}^{6\times 3}.$$

The remainder of the proof consists in showing that the pair $(\boldsymbol{\mathcal{A}}_1(t), \mathbf{C}_1)$ is, indeed, uniformly completely observable. Let $\mathbf{R}_2(t) \in SO(3)$ be a rotation matrix such that

$$\dot{\mathbf{R}}_2(t) = \mathbf{R}_2(t)\mathbf{S}\left[\boldsymbol{\omega}_m(t) - A_{22}\mathbf{x}_1(t)\right].$$

Then, the transition matrix associated with $\boldsymbol{\mathcal{A}}_1(t)$ is given by

$$\boldsymbol{\phi}_1\left(t, t_0\right) = \begin{bmatrix} \mathbf{I} & -\int_{t_0}^{t} \mathbf{R}_2^T\left(\tau\right)\mathbf{R}_2\left(t_0\right)d\tau \\ \mathbf{0} & \mathbf{R}_2^T(t)\mathbf{R}_2\left(t_0\right) \end{bmatrix}.$$

This can be verified since $\boldsymbol{\phi}_1\left(t_0, t_0\right) = \mathbf{I}$ and

$$\frac{d}{dt}\boldsymbol{\phi}_1\left(t, t_0\right) = \boldsymbol{\mathcal{A}}_1(t)\boldsymbol{\phi}_1\left(t, t_0\right)$$

for all $t \geq t_0$. Now, let

$$\mathbf{c} = \begin{bmatrix} \mathbf{c}_1 \\ \mathbf{c}_2 \end{bmatrix} \in \mathbb{R}^6, \quad \mathbf{c}_1, \mathbf{c}_2 \in \mathbb{R}^3,$$

be a unit vector and denote by $\boldsymbol{\mathcal{W}}_1\left(t, t+\delta\right)$ the observability Gramian associated with the pair $(\boldsymbol{\mathcal{A}}_1(t), \mathbf{C}_1)$ on $[t, t+\delta]$. Then,

$$\begin{aligned} \mathbf{c}^T\boldsymbol{\mathcal{W}}_1\left(t, t+\delta\right)\mathbf{c} &= \mathbf{c}^T\int_t^{t+\delta} \boldsymbol{\phi}_1^T\left(\tau, t\right)\mathbf{C}_1^T\mathbf{C}_1\boldsymbol{\phi}_1\left(\tau, t\right)d\tau\mathbf{c} \\ &= \int_t^{t+\delta} \left\|\mathbf{f}_1\left(\tau, t\right)\right\|^2 d\tau \end{aligned}$$

for all $t \geq t_0$, with

$$\mathbf{f}_1\left(\tau, t\right) = \mathbf{c}_1 - \int_t^{\tau} \mathbf{R}_2^T\left(\sigma\right)\mathbf{R}_2\left(t\right)\mathbf{c}_2 d\sigma,$$

$\tau \in [t, t+\delta], t \geq t_0$. Fix $\delta > 0$ and $0 < \epsilon_1 < 1$. Suppose that $\left\|\mathbf{c}_1\right\| \geq \epsilon_1$. Then, for all $t \geq t_0$, one has that $\left\|\mathbf{f}_1\left(t, t\right)\right\| = \left\|\mathbf{c}_1\right\| \geq \epsilon_1$ and, using [35, Proposition 4.2], it follows that there exists $\beta_1 > 0$ such that for all $t \geq t_0$ and all time intervals $[t, t+\delta]$, it is possible to choose $t_i \in [t, t+\delta]$ such that $\mathbf{c}^T\boldsymbol{\mathcal{W}}_1\left(t, t_i\right)\mathbf{c} > \beta_1$, which in turn implies that $\mathbf{c}^T\boldsymbol{\mathcal{W}}_1\left(t, t+\delta\right)\mathbf{c} > \beta_1$. Otherwise, if $\left\|\mathbf{c}_1\right\| < \epsilon_1$, as $\mathbf{c}$ is a unit vector, it follows that it must be $\left\|\mathbf{c}_2\right\| > \sqrt{1-\epsilon_1^2} > 0$. Taking the partial derivative of $\mathbf{f}_1\left(\tau, t\right)$ with respect to τ and evaluating at $\tau = t$ gives

$$\frac{\partial}{\partial\tau}\mathbf{f}_1\left(\tau, t\right)\Big|_{\tau=t} = -\mathbf{c}_2$$

for all $t \geq t_0$ and hence

$$\left\|\frac{\partial}{\partial\tau}\mathbf{f}_1\left(\tau, t\right)\Big|_{\tau=t}\right\| > \sqrt{1-\epsilon_1^2} > 0$$

for all $t \geq t_0$. Then, using [35, Proposition 4.2], it follows that there exists $\beta_2 > 0$ such that, for all $t \geq t_0$ and all time intervals $[t, t+\delta]$, it is possible to choose $t_j \in [t, t+\delta]$ such that $\mathbf{c}^T\boldsymbol{\mathcal{W}}_1\left(t, t_j\right)\mathbf{c} > \beta_2$, which in turn implies that $\mathbf{c}^T\boldsymbol{\mathcal{W}}_1\left(t, t+\delta\right)\mathbf{c} > \beta_2$. Therefore, it was shown that there exists $\beta_3 := \min\left(\beta_1, \beta_2\right) > 0$ such that, for all unit vectors $\mathbf{c}$ and all $t \geq t_0$, it is true that $\mathbf{c}^T\boldsymbol{\mathcal{W}}_1\left(t, t+\delta\right)\mathbf{c} > \beta_3$. This concludes the proof of uniform complete observability of the pair $(\boldsymbol{\mathcal{A}}_1(t), \mathbf{C}_1)$ since both system matrices are bounded, thus concluding the proof of the theorem.

C. Proof of Proposition 1

First, consider the decomposition of the angular velocity of the Earth, $\boldsymbol{\omega}_E(t)$ using the orthonormal basis (12), as given by

$$\boldsymbol{\omega}_E(t) = W_{e1}\mathbf{x}_1(t) + W_{e2}\mathbf{x}_1(t) \times \mathbf{x}_2(t), \qquad (28)$$

see Appendix D for the computations. Then, from (17) and (28) one can write the error of the estimate of the angular velocity of the Earth as

$$\begin{aligned}\tilde{\boldsymbol{\omega}}_E(t) &= W_{e1}\left[\mathbf{x}_1(t)-\hat{\mathbf{x}}_1(t)\right] \\ &\quad +W_{e2}\left[\mathbf{x}_1(t)\times\mathbf{x}_2(t)-\hat{\mathbf{x}}_1(t)\times\hat{\mathbf{x}}_2(t)\right]\end{aligned}$$

and, by definition of the errors $\tilde{\mathbf{x}}_1(t)$ and $\tilde{\mathbf{x}}_2(t)$, it follows that

$$\begin{aligned}\tilde{\boldsymbol{\omega}}_E(t) &= W_{e1}\tilde{\mathbf{x}}_1(t)+W_{e2}\tilde{\mathbf{x}}_1(t)\times\mathbf{x}_2(t) \\ &\quad +W_{e2}\mathbf{x}_1(t)\times\tilde{\mathbf{x}}_2(t)-W_{e2}\tilde{\mathbf{x}}_1(t)\times\tilde{\mathbf{x}}_2(t).\end{aligned} \tag{29}$$

Using simple norm inequalities, one can now write, from (29), that

$$\begin{aligned}\left\|\tilde{\boldsymbol{\omega}}_E(t)\right\| &\leq |W_{e1}|\left\|\tilde{\mathbf{x}}_1(t)\right\|+|W_{e2}|\left\|\mathbf{x}_2(t)\right\|\left\|\tilde{\mathbf{x}}_1(t)\right\| \\ &+|W_{e2}|\left\|\mathbf{x}_1(t)\right\|\left\|\tilde{\mathbf{x}}_2(t)\right\|+|W_{e2}|\left\|\tilde{\mathbf{x}}_1(t)\right\|\left\|\tilde{\mathbf{x}}_2(t)\right\|.\end{aligned} \tag{30}$$

Recall that both $\mathbf{x}_1(t)$ and $\mathbf{x}_2(t)$ have constant norm. Moreover, under the conditions of Theorem 1, both $\tilde{\mathbf{x}}_1(t)$ and $\tilde{\mathbf{x}}_2(t)$ converge globally exponentially fast to zero. Therefore, since the upper bound in (30) consists in a sum of decaying exponentials, it follows that there exists a single decaying exponential that bounds the sum from above, therefore concluding the proof.

D. Decomposition of $\boldsymbol{\omega}_E(t)$ in $\mathcal{B}$

The decomposition of $\boldsymbol{\omega}_E(t)$ in the orthonormal basis (12) is given by

$$\begin{aligned}\boldsymbol{\omega}_E(t) &= \boldsymbol{\omega}_E(t)\cdot\frac{\mathbf{x}_1(t)}{\left\|\mathbf{x}_1(t)\right\|}\frac{\mathbf{x}_1(t)}{\left\|\mathbf{x}_1(t)\right\|} \\ &\quad +\boldsymbol{\omega}_E(t)\cdot\frac{\mathbf{x}_2(t)}{\left\|\mathbf{x}_2(t)\right\|}\frac{\mathbf{x}_2(t)}{\left\|\mathbf{x}_2(t)\right\|} \\ &\quad +\boldsymbol{\omega}_E(t)\cdot\frac{\mathbf{x}_1(t)\times\mathbf{x}_2(t)}{\left\|\mathbf{x}_1(t)\times\mathbf{x}_2(t)\right\|}\frac{\mathbf{x}_1(t)\times\mathbf{x}_2(t)}{\left\|\mathbf{x}_1(t)\times\mathbf{x}_2(t)\right\|}.\end{aligned} \tag{31}$$

The second term of the sum in (31) is null since $\boldsymbol{\omega}_E(t)$ is orthogonal to $\mathbf{x}_2(t)$ (recall that $\mathbf{x}_2(t)=\boldsymbol{\omega}_E(t)\times\mathbf{m}(t)$). Moreover, using the definitions of $\mathbf{x}_1(t)$ and $\mathbf{x}_2(t)$, as well as (5) and (6), and using (1) and (2) in (31) allows one to write

$$\begin{aligned}\boldsymbol{\omega}_E(t) &= \frac{\boldsymbol{\omega}_E(t)\cdot\mathbf{m}(t)}{\left\|{}^I\mathbf{m}\right\|^2}\mathbf{x}_1(t) \\ &\quad +\frac{\boldsymbol{\omega}_E(t)\cdot\left(\mathbf{m}(t)\times\left[\mathbf{m}(t)\times\boldsymbol{\omega}_E(t)\right]\right)}{\left\|{}^I\mathbf{m}\times\left({}^I\boldsymbol{\omega}_E\times{}^I\mathbf{m}\right)\right\|^2}\mathbf{x}_1(t)\times\mathbf{x}_2(t).\end{aligned} \tag{32}$$

Now, substituting (5) and (6) in (32), using the vector triple product and $\mathbf{R}(t)\mathbf{R}^T(t)=\mathbf{I}$, allows to further write

$$\begin{aligned}\boldsymbol{\omega}_E(t) &= \frac{{}^I\mathbf{m}\cdot{}^I\boldsymbol{\omega}_E}{\left\|{}^I\mathbf{m}\right\|^2}\mathbf{x}_1(t) \\ &\quad +\frac{\left[\mathbf{m}(t)\cdot\boldsymbol{\omega}_E(t)\right]^2-\left\|\mathbf{m}(t)\right\|^2\left\|\boldsymbol{\omega}_E(t)\right\|^2}{\left\|{}^I\mathbf{m}\times\left({}^I\boldsymbol{\omega}_E\times{}^I\mathbf{m}\right)\right\|^2}\mathbf{x}_1(t)\times\mathbf{x}_2(t).\end{aligned} \tag{33}$$

Substituting again (5) and (6) in (33), and using the properties (1) and $\mathbf{R}(t)\mathbf{R}^T(t)=\mathbf{I}$, finally gives (28).

E. Proof of Theorem 2

The proof is similar to that of [16, Theorem 3] and as such only a sketch is presented here for the sake of completeness. First, one can show, using the standard quadratic Lyapunov function $V_2\left(\tilde{\mathbf{z}}_2(t)\right)=\frac{1}{2}\left\|\tilde{\mathbf{z}}_2(t)\right\|^2$, that the origin of the unperturbed linear time-varying system $\dot{\tilde{\mathbf{z}}}_2(t)=\mathbf{A}_2(t)\tilde{\mathbf{z}}_2(t)$ is a globally exponentially stable equilibrium point. Next, in a similar way to [33, Example 9.6], one can conclude that the origin of the linear time-varying system

$$\dot{\tilde{\mathbf{z}}}_2(t)=\left(\mathbf{A}_2(t)-\mathbf{S}_3\left[\tilde{\boldsymbol{\omega}}_E(t)\right]\right)\tilde{\mathbf{z}}_2(t) \tag{34}$$

is a globally exponentially stable equilibrium point since, under the conditions of the theorem, $\left\|\mathbf{S}_3\left[\tilde{\boldsymbol{\omega}}_E(t)\right]\right\|$ converges exponentially fast to zero. Finally, notice that (22) corresponds to the linear time-varying system (34) perturbed by an additive disturbance that, in the conditions of the theorem, converges exponentially fast to zero. As such, the origin of (22) is also a globally exponentially stable equilibrium point.